Journal of
Composites Science

MDPI

Article

Composite Building Materials Prepared from Bioresources: Use of Rice Husk for Autoclaved Lightweight Concrete Production

Shao-Lin Peng [1], Ying-Liang Chen [1,*] and Yu-Sheng Dai [2]

[1] Department of Resources Engineering, National Cheng Kung University, Tainan 701, Taiwan; z58101014@gs.ncku.edu.tw
[2] Department of Environmental Engineering, National Cheng Kung University, Tainan 701, Taiwan; p56071159@mail.ncku.edu.tw
* Correspondence: z10808013@ncku.edu.tw; Tel.: +886-6-2757575 (ext. 62831)

Abstract: Rice husk (RH) and straw are common agricultural wastes in Asian countries, and they are potential bioresources for building materials. RH contains a large amount of SiO_2, and many studies have burnt RH to ash and then used it as a silica supplement in cement and concrete. However, the combustion of RH has an additional cost and exacerbates CO_2 emissions and air pollution. RH inherently has a low bulk density and porous structure; therefore, it should be possible to directly use RH as a lightweight additive in concrete. The purposes of this study were to use RH in the production of autoclaved lightweight concrete (ALC) and to examine the effects of RH on ALC properties. Four RHs with different particle sizes, i.e., >1.2 mm, 0.6–1.2 mm, 0.3–0.6 mm, and <0.3 mm, were used as lightweight additives, and the ALC specimens were prepared with 0–20 wt.% RHs by autoclaving at 189 °C for 12 h. The >0.3 mm RH was applicable to prepare the ALC specimens, and the decomposition effect of <0.3 mm RH was significant. Both the bulk density and the compressive strength of the ALC specimens decreased with increasing RH size. RH with a particle size larger than 1.2 mm seems more appropriate for ALC production than RH with a smaller particle size because of the lower bulk density and higher compressive strength. The Ca/Si ratio decreased with increasing RH size, which affected the formation of tobermorite and thus reduced the compressive strength of the ALC specimens. With a suitable water-to-solid (W/S) ratio, the use of RHs as lightweight additives can yield ALC specimens that meet the requirements of commercial products.

Keywords: rice husk; autoclaved lightweight concrete; agricultural waste; bioresource; compressive strength; bulk density; performance factor

Citation: Peng, S.-L.; Chen, Y.-L.; Dai, Y.-S. Composite Building Materials Prepared from Bioresources: Use of Rice Husk for Autoclaved Lightweight Concrete Production. *J. Compos. Sci.* **2024**, *8*, 359. https://doi.org/10.3390/jcs8090359

Academic Editor: Yanshuai Wang

Received: 12 August 2024
Revised: 7 September 2024
Accepted: 11 September 2024
Published: 13 September 2024

1. Introduction

Rice cultivation is predominantly concentrated in Asian countries, and rice serves as a primary staple food for Taiwanese people. In 2023, the rice cultivation area in Taiwan reached 222,000 ha, yielding 1.46 million tons of paddy rice. During the rice production process, large amounts of crop residues, such as rice husk (RH) and straw, are generated. In Taiwan, 292,074 tons of RH, which accounts for ~20 wt.% of paddy rice, were generated in 2023 [1]. The main components of RH are approximately 80% organic substances (e.g., cellulose, hemicellulose, and lignin) and 20% inorganic substances, most of which are silica. RH also has several unique characteristics including a low bulk density, high specific surface area, and porous structure [2–5].

Historically, in the early 20th century, RH was used as an additive to building materials in Taiwan when agriculture was the main economic activity. Traditional Taiwanese architecture often uses a composite of RH and clay to create adobes in house construction [6]. With the development of building materials and engineering technology, the adobes have become historical monuments, and RH is no longer used in modern building materials. In

recent years, many researchers have studied the use of rice husk ash (RHA) in concrete materials [7–12]. RHA is produced by burning RH with sufficient oxygen. The organic substances of RH are completely removed, and RHA containing high-purity silica is thus obtained. RHA can be used as a pozzolanic material in concrete, and many studies indicate that the use of RHA can increase the compressive strength and durability of concrete materials [7,8,11]. However, the combustion of RH increases CO_2 emissions and causes air pollution [13,14]. In addition, rice husk biochar (RHB) and rice straw have been used in building materials [15–17]. Muthukrishnan et al. [17] converted RH to RHB and then used it in cement mortar to improve the mechanical strength and durability. The addition of RHB also significantly reduced the autogenous shrinkage of the cement mortar. Pachla et al. [16] used rice straw in cellular concrete and reported that the rice straw increased the three-point bending strength but decreased the compressive strength. Moreover, the rice straw improved the sound and heat insulation of the resultant cellular concrete. The Taiwan government has been committed to developing a circular economy in recent years, and one of the related policies is to advance the treatment and recycling technologies for agricultural wastes [18]. Previous studies indicate that wastes derived from rice cultivation should have the potential to be used in concrete materials.

Owing to its low bulk density, high silica content, and porous nature, RH is suitable for the development of lightweight concrete products, such as autoclaved lightweight concrete (ALC). ALC is a lightweight precast component created by evenly distributing air bubbles within concrete via the addition of lightweight materials, foaming agents, or gases. ALC typically has a thermal conductivity between 0.2 and 1.0 W/m·K and a bulk density ranging from 0.3 to 1.8 g/cm^3, which is approximately 25% that of conventional concrete [19–21]. Compared with conventional concrete, ALC has low thermal conductivity, excellent sound and heat insulation, and fire resistance, and it has a wide range of applications [19,22,23]. Some studies have indicated that the use of RH as a substitute in ALC production can not only reduce the bulk density but also improve the mechanical strength and durability. During ALC production, the silica from RH can react with $Ca(OH)_2$ to form calcium silicate hydrates (CSHs), and the transformation of CSHs into tobermorite during autoclave curing could improve the mechanical strength and durability [24,25].

The formation of tobermorite is closely related to the Ca/Si molar ratio in the material. Optimal tobermorite formation occurs when the Ca/Si molar ratio is between 0.8 and 1.0. Moreover, different Ca/Si molar ratios affect the structural characteristics of tobermorite. Generally, tobermorite in plate form provides greater mechanical strength than tobermorite in needle form [26,27]. However, some studies have reported that the mechanical strength of the materials decreases as the proportion of RH increases [28,29], which could be attributed to several factors. The use of RH increased the porosity of the composite, compromising the overall structural integrity [30]. Moreover, the composite specimens exhibited high water absorption and air content. This can potentially lead to insufficient hydration reactions and consequently reduce the mechanical strength [31]. Doumongue et al. [32] indicated that the distribution and bonding of RHs within a composite are other crucial factors for maintaining mechanical strength. Chabannes et al. [33] also suggested that the relatively lower stiffness and greater deformability of RHs further contribute to the reduction in mechanical strength.

Given the aforementioned challenges, the aim of this research is to optimize the use of RH in ALC production to increase structural integrity and performance. In the experimental work, the characteristics of raw RH were examined first, and the raw RH was then separated into four particle sizes for further analyses and experiments. The RHs with different particle sizes were used for ALC production, and the effects of the RH amount and water-to-solid (W/S) ratio on the properties of the ALC specimens were studied.

2. Materials and Methods

The raw RH was obtained from a rice mill in southern Taiwan. To examine the characteristics of raw RH, proximate analysis (moisture content, loss on ignition (LOI), and

ash content), chemical composition analysis, X-ray diffraction (XRD) analysis, and particle size analysis were conducted. The moisture content was determined by drying the RH at 105 °C for 24 h to obtain the weight loss of water. LOI was measured by calcining the RH at 850 °C for 3 h. The residual weight after the LOI measurement was used to calculate the ash content. The chemical composition of the RH was determined via an X-ray fluorescence (XRF) spectrometer (XEPOS, Spectro, Kleve, Germany). The XRD analysis was conducted by using an X-ray diffractometer (D8 Advance, Bruker, Karlsruhe, Germany) with Cu-Kα radiation. The XRD patterns were recorded between 5°2θ and 65°2θ with a scanning step of 0.02°. Before the XRF and XRD analyses, the RH was dried and ground into a powder with a particle size less than 0.075 mm. The particle size analysis for the RH was conducted by using a test sieve shaker (AS 200 Basic, Retsch, Haan, Germany) with standard test sieves of 0.075 mm, 0.15 mm, 0.3 mm, 0.6 mm, 1.2 mm, and 2.4 mm.

To obtain RHs with different particle sizes for the production of ALC, the RH was shredded with a pulverizing machine (RT-02A, Rong Tsong Precision Technology Co., Taichung, Taiwan) and then separated into four particle sizes, namely, RH-L (>1.2 mm), RH-M (0.6–1.2 mm), RH-S (0.3–0.6 mm), and RH-F (<0.3 mm). Photos of these RHs are shown in Figure 1. It was observed that most of the >1.2 mm particles (RH-L) were intact RH. In contrast, RH-F (<0.3 mm) was a fine powder, and few features of RH remained. For the preparation of ALC specimens, slaked lime ($Ca(OH)_2$, 97.8%, Schaefer Kalk, Diez, Germany), silica powder (SiO_2, 99.5%, Alfa Aesar, Ward Hill, MA, USA), and cement (Taiwan Cement Corporation, Taipei, Taiwan) were employed as the ALC raw materials in this study. The weight percentages of slaked lime, silica powder, and cement were 45.0 wt.%, 45.0 wt.%, and 10.0 wt.%, respectively. Table 1 shows the chemical compositions of the ALC raw materials.

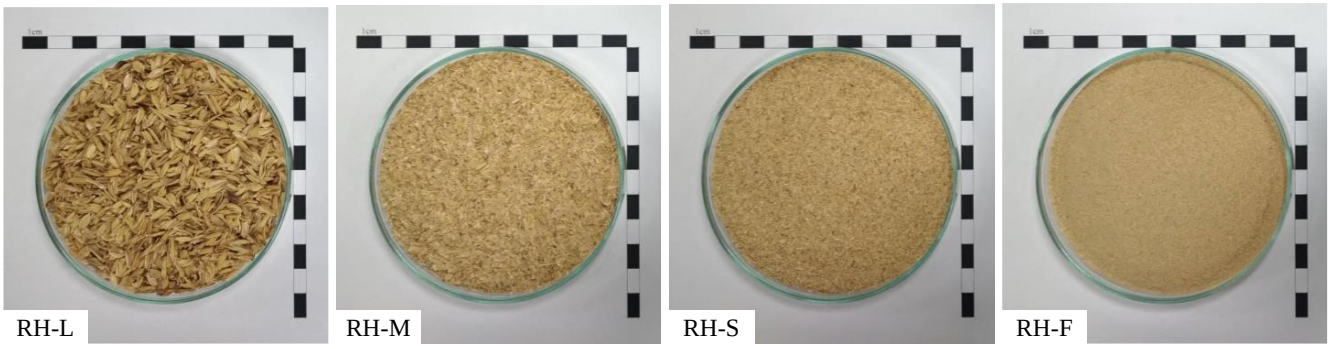

Figure 1. Photos of RHs with different particle sizes.

Table 1. Chemical compositions of ALC raw materials.

Chemical Composition	Slaked Lime [1]	Silica Powder [1]	Cement [1]
Mg (wt.%)	0.36	0.004	1.61
Al (wt.%)	0.04	0.470	2.56
Si (wt.%)	0.06	46.51	14.47
P (wt.%)	NA [2]	NA [2]	NA [2]
S (wt.%)	0.01	NA [2]	0.89
Cl (wt.%)	NA [2]	NA [2]	NA [2]
K (wt.%)	NA [2]	NA [2]	0.29
Ca (wt.%)	52.91	0.001	42.12
Fe (wt.%)	0.03	0.029	2.46

[1] Data provided by the manufacturers. [2] NA: not available.

The RHs (RH-L, RH-M, RH-S, and RH-F) were used as lightweight additives, and the amounts of RH were between 0 wt.% and 20 wt.%. The raw materials and RHs were mixed together with a rotary agitator for 30 min and then put into a mixing bowl. Water was added to the raw mixture at a specific W/S ratio (0.7–0.8 L/kg) and then blended

into slurry with an electric blender. The slurry was poured into 50 mm cubic molds where it was allowed to expand. The expansion of the slurry nearly finished after standing for 30 min, and the bump on the top of the molds was removed. The molds were then moved into a moist closet for precuring, in which the temperature was 23 ± 2 °C and the relative humidity was ≥95%. After precuring for 24 h, the hardened specimens were obtained and the molds were subsequently removed. The hardened specimens were cured with an autoclave for 12 h to promote hydration reactions. The autoclave curing temperature was set at 189 °C, and the pressure of the saturated steam reached approximately 12 atm. The ALC specimens were prepared and then dried at 105 °C for 24 h before further testing. The bulk density and compressive strength of the ALC specimens were measured according to ASTM C1693. The compressive strength was determined with an electric testing machine (HCH-239-20T, Jin Ching Her Co., Ltd., Yunlin, Taiwan) at a loading rate of 1.0 mm/min. The water absorption test for the ALC specimens was conducted according to CNS 619. The dried ALC specimens were weighed (W_d) and then immersed in boiling water for 3 h. After cooling to room temperature, the specimens were taken out of the water, and the water attached to the surfaces was removed. The specimens saturated with water were weighed (W_s), and the water absorption percentage was obtained via Equation (1).

$$\text{Water absorption}(\%) = \frac{W_s(g) - W_d(g)}{W_d(g)} \times 100\% \quad (1)$$

The scheme of the full experimental setup is presented in Figure 2.

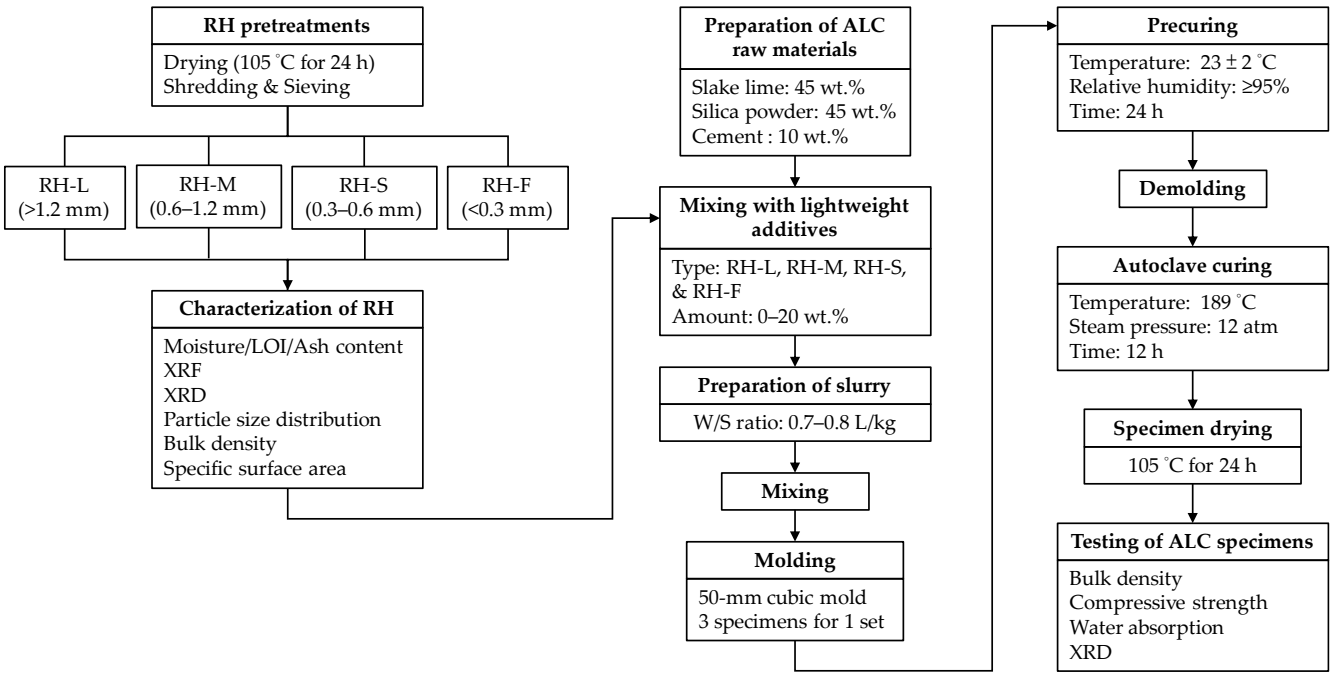

Figure 2. Scheme of the full experimental setup.

3. Results and Discussion

3.1. Characterization of RH

Table 2 shows the moisture content, LOI, and ash content of the RH samples. The RH originally contained 11.19 wt.% moisture, which is close to the typical upper bound reported in a previous study [34]. The RH had a high LOI (76.73 wt.%) and contained 12.08 wt.% ash at 850 °C under an air atmosphere for 3 h. The LOI should be attributed to the combustion of organic substances, such as cellulose, hemicellulose, and lignin. RHA is a combustion residue of RH, and many studies have indicated that RHA is mainly composed of SiO_2 [35,36]. Because the moisture content of RH usually fluctuates depending on the

storage environment and time, it is more useful to use the dry-basis LOI and ash content for comparison with other studies. The dry-basis ash content of the RH in this study was 13.61 wt.%, which is slightly lower than most of the values reported by Jittin et al. [37]. The soil environment for paddy rice should be the key factor that affects the ash content of RH.

Table 2. Moisture content, LOI, and ash content of the RH.

Percentage	Moisture Content	LOI [1]	Ash Content
wt.%	11.19	76.73	12.08
wt.% (dry basis)	–	86.39	13.61

[1] LOI: loss on ignition (at 850 °C for 3 h).

The chemical composition of the RH is given in Table 3. Notably, Si accounted for 11.79 wt.% of the RH, a value that is much higher than those of the other elements. In addition to Si, K was detected at 1.54 wt.%, and Mg, P, Ca, S, and Cl were found at approximately 0.20–0.50 wt.%. Some trace metals, including Mn (126 mg/kg), Ba (40 mg/kg), Ti (24 mg/kg), Zn (22 mg/kg), and Ni (11 mg/kg), were also present in the RH. Jauberthie et al. [25] observed the distribution of Si in RH and reported that Si existed as amorphous silica and was concentrated on the surfaces of RH, not within the RH itself.

Table 3. Chemical composition of the RH.

Chemical Composition		RH
Major Element (wt.%)	Mg	<0.50
	Al	<0.01
	Si	11.79
	P	0.29
	S	0.20
	Cl	0.20
	K	1.54
	Ca	0.23
	Fe	0.03
Trace Metal (mg/kg)	Ti	24
	Mn	126
	Ni	11
	Zn	22
	Ba	40

Figure 3 presents the XRD pattern of the RH. The diffraction intensity of the pattern was very low, which showed that the RH was nearly amorphous. Only a weak peak related to silicon oxide (SiO_2) was identified in the XRD pattern of RH. Figure 4 shows the particle size distributions of the RH and the shredded RH. The RH originally had small amounts of <1.2 mm particles. The particle size of 0.6–1.2 mm was 10.57 wt.%, and the individual weight percentages of the smaller particles were all less than 3.5 wt.%. A particle size of >1.2 mm accounted for more than 82 wt.% of the RH. To prepare RHs with different particle sizes, it was necessary to shred the RH. After shredding, the <0.3 mm particles increased to 37.72 wt.%, and the 0.3–0.6 mm and 0.6–1.2 mm particles were 36.59 wt.% and 23.53 wt.%, respectively. Accordingly, four RHs with different particle sizes, i.e., RH-L (>1.2 mm), RH-M (0.6–1.2 mm), RH-S (0.3–0.6 mm), and RH-F (<0.3 mm), were prepared for the subsequent experiments.

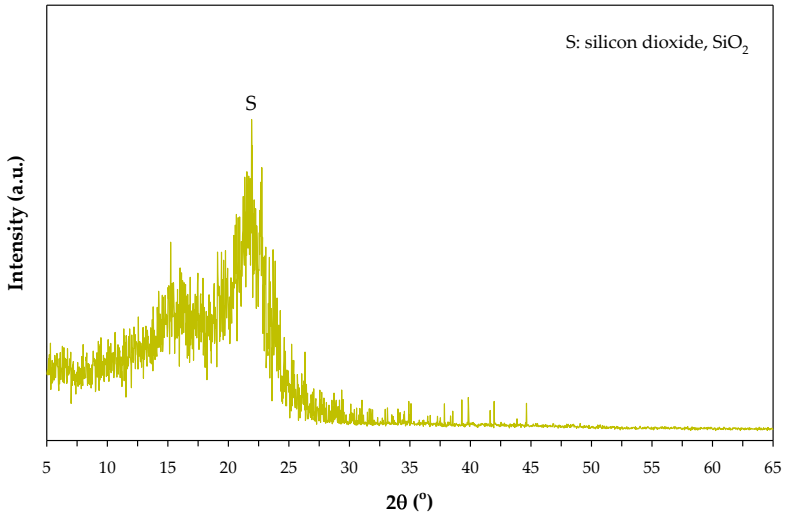

Figure 3. XRD pattern of the RH.

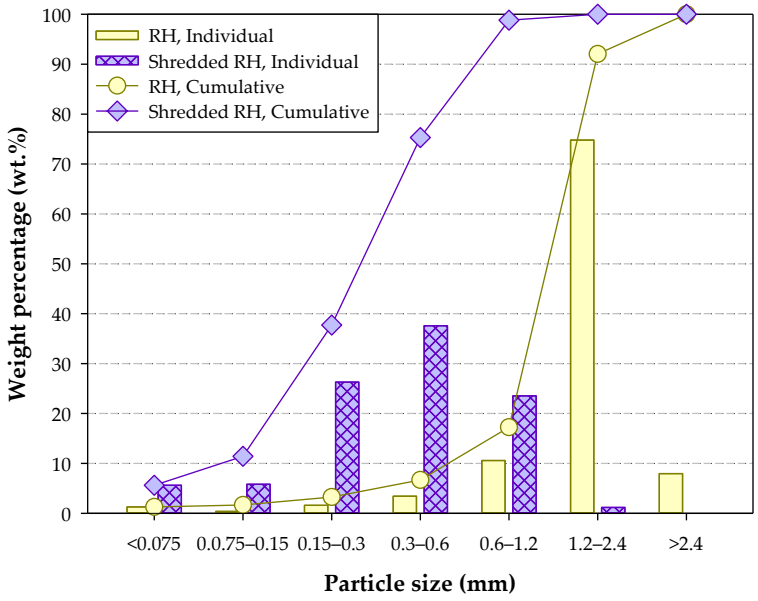

Figure 4. Particle size distributions of the RH and the shredded RH.

Table 4 lists the bulk density and specific surface area of RH-L, RH-M, RH-S, and RH-F. The bulk density of RH-L was only 0.102 g/cm^3; as the particle size decreased, the bulk density of the RHs increased. The bulk density of RH-F reached 0.456 g/cm^3. Because RHs were used as lightweight additives for ALC production, a lower bulk density should be more appropriate. The specific surface area of RHs also varied with the particle size. The specific surface area of RH-L was only 43.4 m^2/kg, whereas that of RH-F was 768.5 m^2/kg. A high specific surface area could increase water adsorption on surfaces and change the effects of RHs on ALC properties.

Table 4. Bulk density and specific surface area of the RHs with different particle sizes.

Characteristic	RH-L	RH-M	RH-S	RH-F
Particle size (mm)	>1.2	0.6–1.2	0.3–0.6	<0.3
Bulk density (g/cm^3)	0.102	0.276	0.354	0.456
Specific surface area (m^2/kg)	43.4	91.1	139.3	768.5

3.2. Properties of ALC Prepared with RHs

Figure 5 shows photos of the ALC specimens prepared with RH-L, RH-M, RH-S, and RH-F. When the amounts of RHs increased, the surfaces of the ALC specimens became rougher, and more voids and cracks were observed. The color of the ALC specimens also became darker when increasing the amounts of RHs. It was noted that RH-F failed in the preparation of ALC specimens. The ALC specimen prepared with 4 wt.% RH-F had large cracks and that prepared with 12 wt.% RH-F broke in half. Therefore, RH-F was excluded from the subsequent experiments. Jittin et al. [37] reported that RH contained 11.96–31.68 wt.% hemicellulose and 26.20–35.62 wt.% cellulose. Compared with cellulose, hemicellulose can be hydrolyzed more easily under acidic or basic conditions. The hydrolysis of hemicellulose could occur during ALC production, thus affecting the properties of the ALC specimens. Moreover, RH-F was a fine powder with a high specific surface area, and the effects of hydrolysis reactions should be more significant.

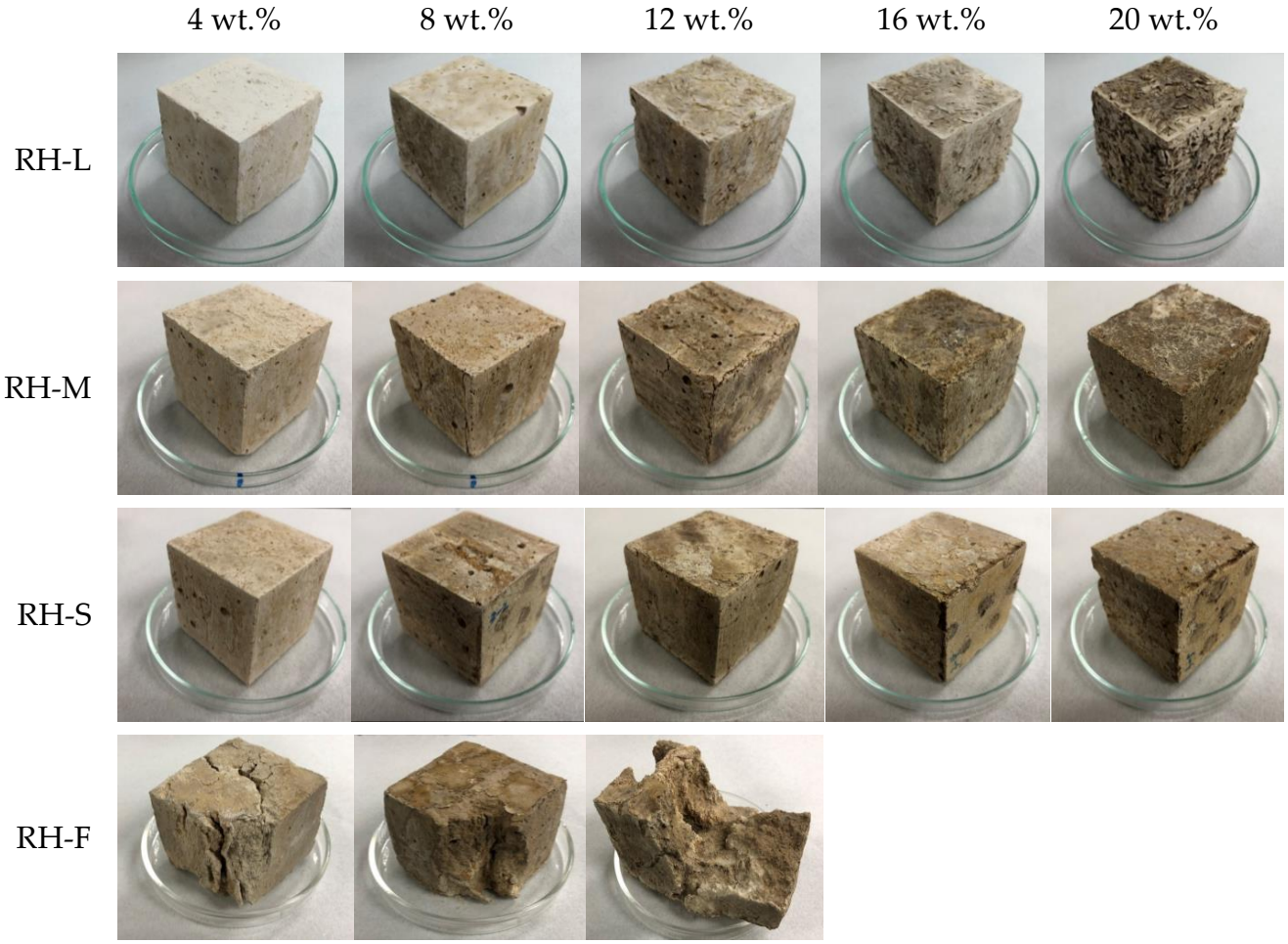

Figure 5. Photos of the ALC specimens prepared with RHs with different particle sizes.

Figure 6 presents the bulk density of the ALC specimens prepared with RH-L, RH-M, and RH-S. Generally, the bulk density of the ALC specimens gradually decreased with increasing RH size. The ALC specimens prepared with RH-L had a lower bulk density than those prepared with RH-M or RH-S. However, the difference in the bulk density of ALC specimens between RHs was not very significant.

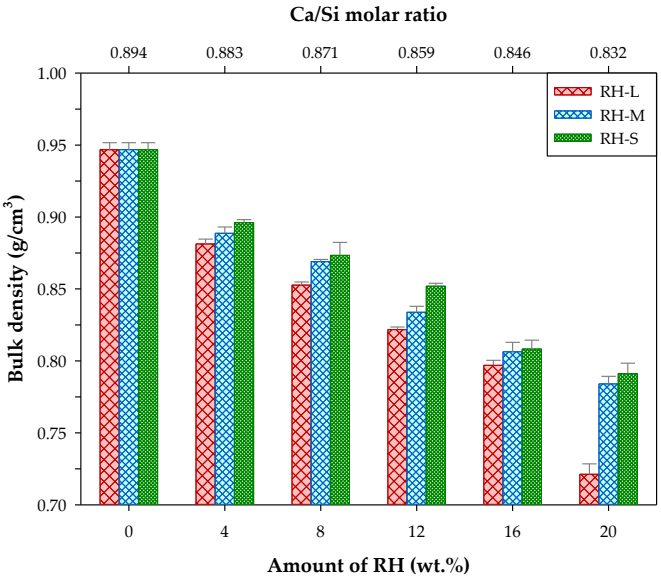

Figure 6. Bulk density of the ALC specimens prepared with RH-L, RH-M, and RH-S.

The compressive strength of the ALC specimens prepared with RH-L, RH-M, and RH-S is shown in Figure 7. When RHs were used as lightweight additives, the compressive strength of the ALC specimens significantly decreased with increasing RH size. At a specific amount of RH, the ALC specimens prepared with RH-L mostly had higher compressive strength than those prepared with RH-M or RH-S. The decrease in compressive strength of the ALC specimens may be due to the change in the Ca/Si molar ratio. The initial Ca/Si molar ratio was 0.849 when no RHs were added. The Ca/Si molar ratio decreased with the amount of RH added because additional Si was introduced with RHs. The Ca/Si molar ratio decreased to 0.832 when 20 wt.% RHs was used for ALC production. Many studies have indicated that the Ca/Si molar ratio is highly related to the formation of tobermorite and the development of compressive strength [26,27,38,39].

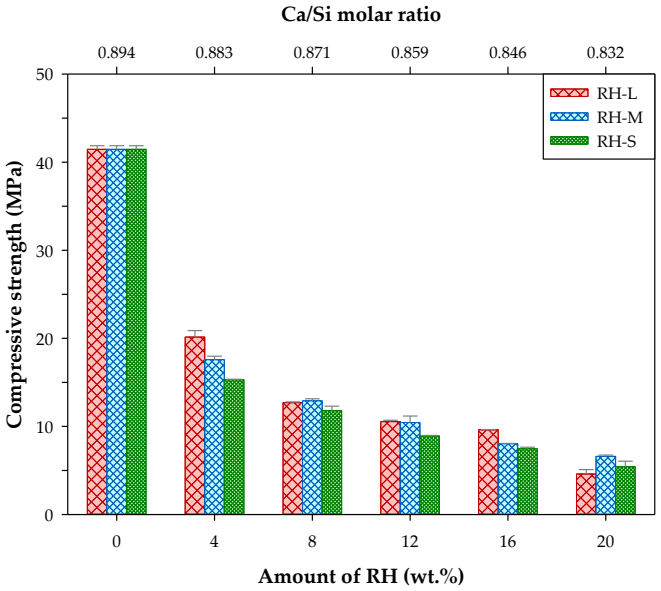

Figure 7. Compressive strength of the ALC specimens prepared with RH-L, RH-M, and RH-S.

The performance factor (P_f) has been used by many researchers to evaluate the combined performance of a lightweight material (e.g., ALC and foamed concrete) because the variation in the compressive strength is highly related to that in the bulk density [40–42].

The calculation of the P_f value is shown in Equation (2). Figure 8 shows the P_f values of the ALC specimens prepared with RH-L, RH-M, and RH-S. The P_f values of ALC specimens generally decreased with increasing RH size. Notably, the ALC specimens prepared with RH-L had higher P_f values than those prepared with RH-M or RH-S. These findings indicate that that RHs with larger particle sizes are more appropriate lightweight additives for ALC production. The ALC specimens prepared with 12 wt.% RH-L had relatively stable P_f values, and the bulk density reduced to 0.822 g/cm^3. Therefore, the use of 12 wt.% > 1.2 mm RH is the optimal condition for the production of ALC.

$$P_f(\text{MPa/g/cm}^3) = \frac{\text{Compressive strength(MPa)}}{\text{Bulk density(g/cm}^3)} \quad (2)$$

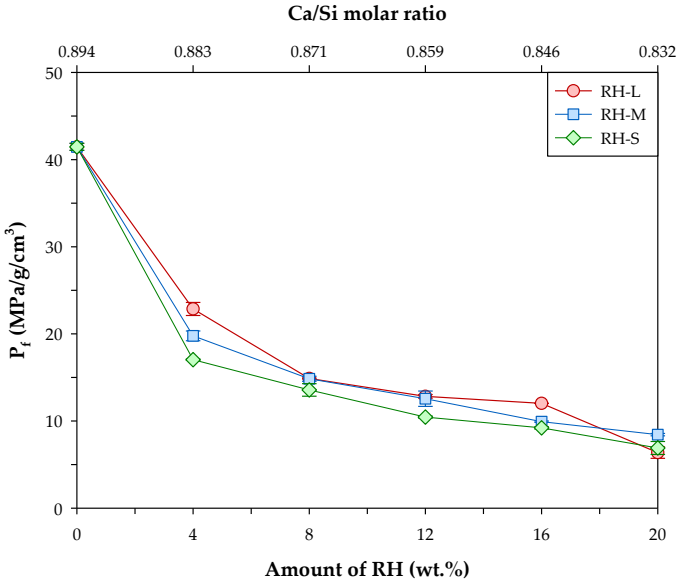

Figure 8. P_f values of the ALC specimens prepared with RH-L, RH-M, and RH-S.

The XRD patterns of the ALC specimens prepared with RHs are presented in Figure 9. In the ALC specimen prepared without RHs, tobermorite was the main crystalline phase, and quartz (SiO_2) barely existed. When RHs were used as lightweight additives, the diffraction intensity of tobermorite decreased and quartz appeared in the ALC specimens. It was also found that at a specific amount of RH, the ALC specimens prepared with RH-M and RH-S had higher diffraction intensities of quartz than that prepared with RH-L. Chandrasekhar et al. [12] indicated that the SiO_2 in RH is present in a hydrated amorphous form, which has high reactivity, and it can convert to crystalline forms during thermal treatment. Another possible situation is that the high-reactivity SiO_2 from RH may react with $Ca(OH)_2$ first to form tobermorite, thus causing the added silica powder to remain in the ALC specimens. These findings showed that an excess of SiO_2 was provided by the RHs, especially for RHs with small particle sizes, and thus affected the formation of tobermorite. With increasing RH size, the effect of RHs on the formation of tobermorite became more significant and was likely responsible for the decrease in the compressive strength of the ALC specimens. Liu et al. [38] concluded that an ideal Ca/Si molar ratio can maximize the formation of tobermorite and enhance the compressive strength. In this study, the Ca/Si molar ratio decreased due to the excess SiO_2 provided by the RHs and therefore interfered with the tobermorite formation and compressive strength.

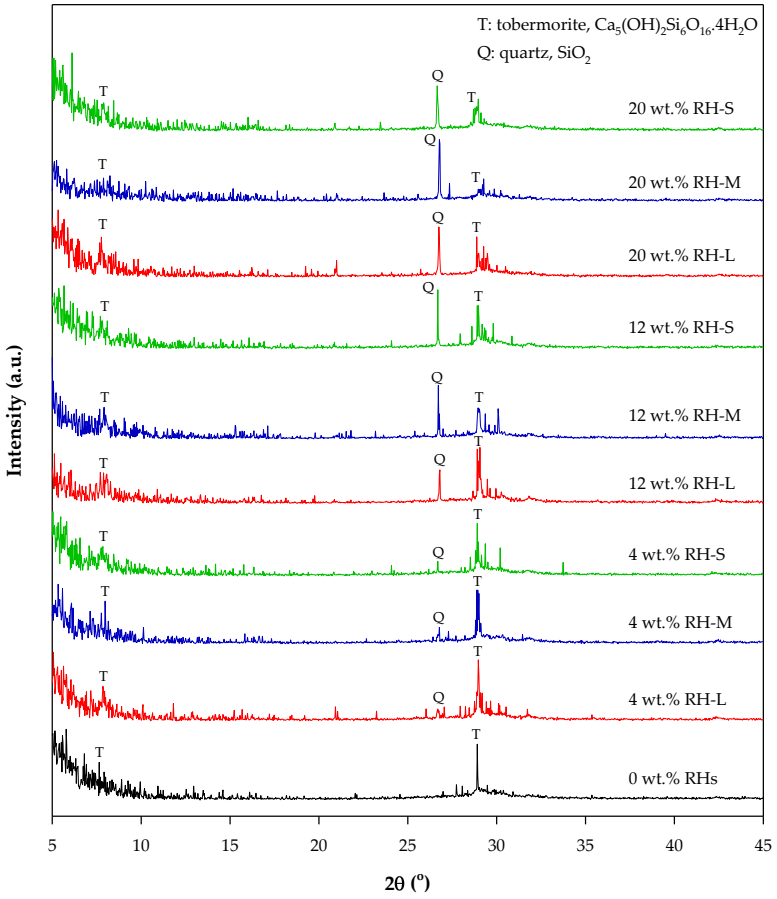

Figure 9. XRD patterns of the ALC specimens prepared with RHs.

Table 5 shows the water absorption of the ALC specimens prepared with RHs. In general, the water absorption was negatively related to the bulk density of the ALC specimens (compared to Figure 6). For typical building materials, water absorption could be limited to a certain level, especially when the impact of water freezing and thawing is considered. Rahman et al. [43] noted that water absorption is contributed by capillary pores (<1 μm) and large ventilation pores. In addition, open pores contribute to water absorption, whereas closed pores do not. The ALC specimens prepared with RH-L had greater water absorption than the other specimens did. However, the ALC specimens prepared with 4–12 wt.% RH-L had relatively low water absorption (76.2–78.2 wt.%). High amounts of RH-L (16 wt.% and 20 wt.%) greatly increased the water absorption of the ALC specimens. Therefore, limiting the amount of RH added may be necessary to control the water absorption of ALC.

Table 5. Water absorption of the ALC specimens prepared with RHs.

Amount of RH (wt.%)	Water Absorption (wt.%)		
	RH-L	RH-M	RH-S
4	76.2	70.9	71.7
8	78.6	72.9	73.9
12	78.2	76.7	77.5
16	85.5	79.4	83.7
20	96.0	82.5	84.0

3.3. Effects of the W/S Ratio on the Physical Properties of the ALC Specimens

In addition to lightweight additives, the W/S ratio is also an important parameter for determining the properties of ALC specimens. Water is an essential element of ALC because it promotes the hydration reactions of raw materials and greatly affects the flowability of the ALC slurry. The flowability normally increases with increasing W/S ratio, while the bulk density of the resulting ALC usually decreases [44,45]. Figure 10 illustrates the variation in the bulk density of ALC specimens prepared with RHs at various W/S ratios. The bulk density of the ALC specimens decreased with increasing W/S ratio, as expected. For RH-M (Figure 10b) and RH-S (Figure 10c), the bulk density of the ALC specimens rapidly decreased with increasing W/S ratio and RHs. At higher amounts of RHs, the effect of the W/S ratio on the bulk density of the ALC specimens was more significant. However, when RH-L was used as a lightweight additive (Figure 10a), the effect of the W/S ratio on the bulk density of the ALC specimens seemed more insignificant. The bulk density varied within a relatively narrow range of 0.63–0.89 g/cm^3.

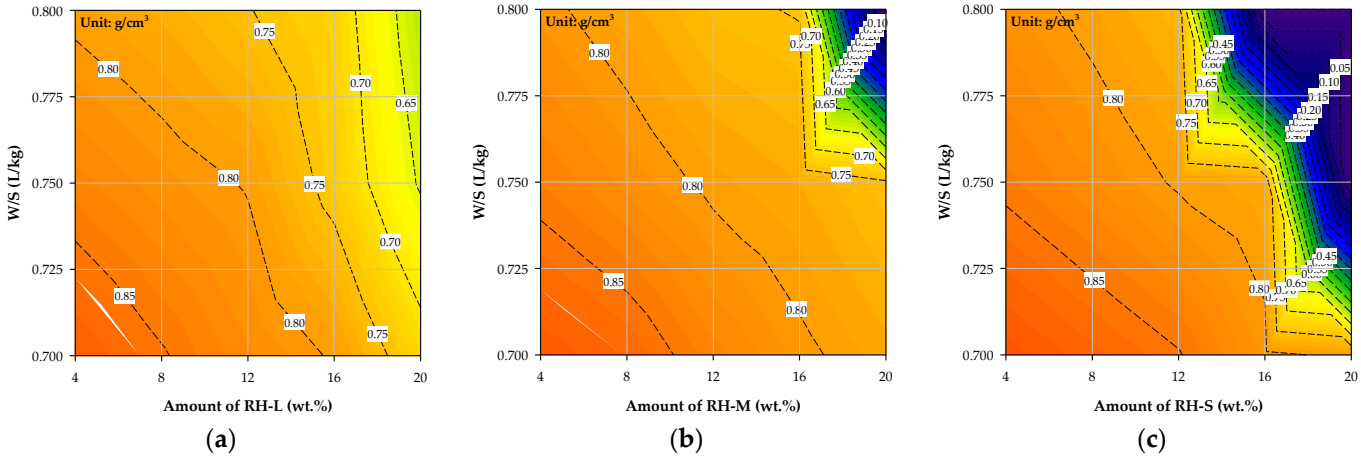

Figure 10. Bulk density of the ALC specimens prepared with the RHs at various W/S ratios: (**a**) RH-L; (**b**) RH-M; (**c**) RH-S.

The compressive strength of ALC specimens prepared with RHs at various W/S ratios is presented in Figure 11. The effect of the RH amount on the compressive strength of the ALC specimens seems greater than that of the W/S ratio. At a specific amount of RH, the increase in the W/S ratio only slightly reduced the compressive strength of the ALC specimens. This result is in line with previous research [46]. It is known that RHs can absorb some water, and this may partially neutralize the increases in the W/S ratio. In comparison, the ALC specimens prepared with RH-L had higher compressive strength at a specific W/S ratio than those prepared with RH-M or RH-S. Chabannes et al. [33] also used RH in lightweight insulating concrete, and the 60-day compressive strength was only 0.33 MPa. The autoclave curing used in this study can significantly increase the compressive strength of the lightweight concrete prepared with RH.

In Taiwan, the properties of qualified ALC products should meet the requirements of the CNS 13480 standard [47]. There are five strength classes of ALC blocks (namely G2, G4, G6, G8, and G10) according to the requirements of compressive strength and bulk density, which are listed in Table 6. The strength class of G10 requires the highest compressive strength (12.5 MPa) and is also allowed to have a maximum bulk density (1.20 g/cm^3). Based on the test results of compressive strength and bulk density, the ALC specimens prepared with RHs can be classified into various strength classes according to CNS 13480, as shown in Figure 12. The ALC specimens prepared with RH-L, RH-M, and RH-S can meet the requirements of G6, G8, and G10 when using appropriate W/S ratios. In this study, ALC specimens compliant with the strength classes of G2 and G4 were not obtained because of the excessive bulk density. When RH-L is used as a lightweight additive, the qualified

ALC specimens can be prepared with 4–16 wt.% RH-L at W/S ratios of 0.70–0.80 L/kg. The ALC specimen prepared with 4 wt.% RH-L at a W/S ratio of 0.80 L/kg can meet all the requirements of G6, G8, and G10, which means that it should have a wide range of applications. The amount of RH-M or RH-S used for ALC production should be restricted to 12 wt.% and less to obtain qualified ALC products.

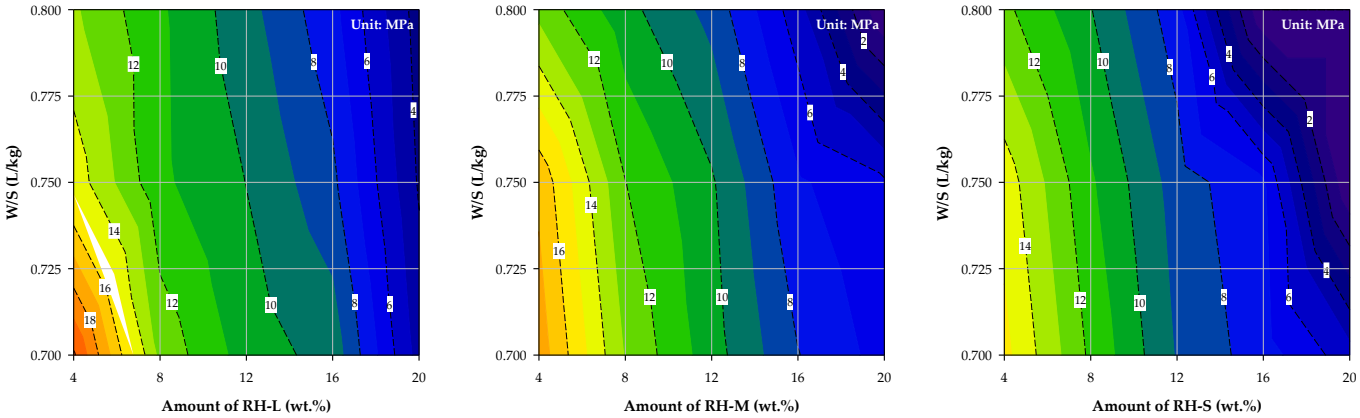

Figure 11. Compressive strength of the ALC specimens prepared with the RHs at various W/S ratios: (**a**) RH-L; (**b**) RH-M; (**c**) RH-S.

Table 6. Physical requirements of the ALC products regulated in CNS 13480.

Strength Class	Compressive Strength (MPa) [1]	Bulk Density (g/cm^3) [2]
G2	2.5	0.50
G4	5.0	0.60
G6	7.5	0.80
G8	10.0	1.00
G10	12.5	1.20

[1] Average of testing specimens, minimum. [2] Dry bulk density, maximum.

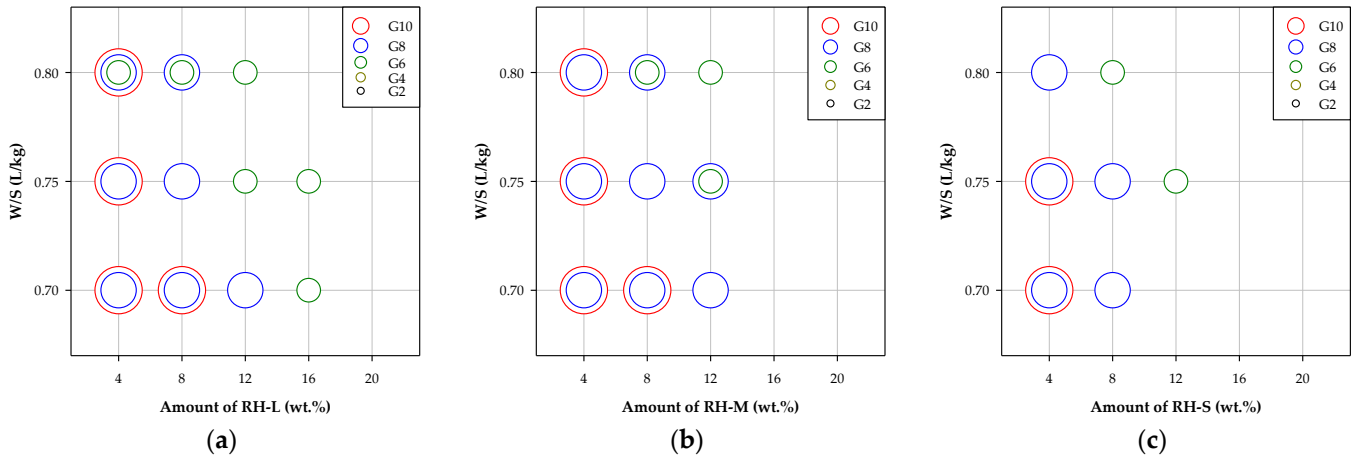

Figure 12. Strength classes of the ALC specimens prepared with the RHs: (**a**) RH-L; (**b**) RH-M; (**c**) RH-S.

4. Conclusions

The following conclusions can be drawn from the present findings of this study:

1. The dried RH had a high LOI (~86 wt.%), which should be attributed to organic substances, and contained ~14 wt.% ash (mostly composed of silica). The particles

larger than 1.2 mm accounted for >82 wt.% of the RH and most of these particles were intact RHs. Four RHs with different particle sizes, namely RH-L (>1.2 mm), RH-M (0.6–1.2 mm), RH-S (0.3–0.6 mm), and RH-F (<0.3 mm), were investigated, and it was found that both the bulk density and the specific surface area increased with the increase in the particle size of the RHs.

2. When RHs were used as lightweight additives for ALC production, the use of RH-F (<0.3 mm) failed to produce ALC specimens. This shows that the decomposition of RHs will occur during the preparation of ALC specimens, and the influence is more significant for RHs with fine particle sizes. Generally, the ALC specimens prepared with RH-L (>1.2 mm) had lower bulk density and higher compressive strength than those prepared with RH-M or RH-S. The bulk density and compressive strength of the ALC specimens simultaneously decreased with increasing RH size. When the amounts of RHs increased, the Ca/Si molar ratio decreased and more SiO_2 remained in the ALC specimens. The formation of tobermorite was thus retarded, causing a reduction in the compressive strength of ALC.
3. The amount of RH may be restricted to a level in order to control the water absorption of the ALC specimens. The effect of the W/S ratio on the bulk density of ALC specimens seems more significant than that on the compressive strength. By appropriately controlling the W/S ratio and the amounts of RHs added, the resulting ALC specimens can meet the requirements of some strength classes for qualified commercial products (CNS 13480: G6, G8, and G10).
4. The above findings prove the feasibility of using RH in the production of ALC. The hydrolysis reactions of cellulose and hemicellulose under autoclaving conditions may be studied in future work to reveal the effects of the hydrolysis products on tobermorite formation and ALC properties.

Author Contributions: Conceptualization, Y.-L.C.; methodology, Y.-L.C.; validation, Y.-L.C.; formal analysis, Y.-S.D.; investigation, Y.-S.D. and S.-L.P.; data curation, Y.-S.D. and S.-L.P.; writing—original draft preparation, S.-L.P. and Y.-L.C.; writing—review and editing, Y.-L.C.; supervision, Y.-L.C.; project administration, Y.-L.C.; funding acquisition, Y.-L.C. All authors have read and agreed to the published version of the manuscript.

Funding: This research was funded by the National Science and Technology Council (NSTC), Taiwan (Contract No.: 112-2221-E-006-044).

Data Availability Statement: The data presented in this study are available on request.

Acknowledgments: The authors graciously thank Juu-En Chang for providing research suggestions and the analysis instruments, such as DSC-TGA, ICP-OES, etc.

Conflicts of Interest: The authors declare no conflicts of interest. The funders had no role in the design of the study; in the collection, analyses, or interpretation of data; in the writing of the manuscript; or in the decision to publish the results.

References

1. Ministry of Agriculture. *2023 Basic Agriculture Statistics*; Ministry of Agriculture: Taipei, Taiwan, 2024.
2. Ma'ruf, A.; Pramudono, B.; Aryanti, N. Lignin isolation process from rice husk by alkaline hydrogen peroxide: Lignin and silica extracted. In Proceedings of the 14th International Symposium on Therapeutic Ultrasound, Las Vegas, NV, USA, 2–5 April 2014; p. 020013.
3. Moayedi, H.; Aghel, B.; Abdullahi, M.a.M.; Nguyen, H.; Rashid, A.S.A. Applications of rice husk ash as green and sustainable biomass. *J. Clean. Prod.* **2019**, *237*, 117851. [CrossRef]
4. Moraes, C.A.M.; Fernandes, I.J.; Calheiro, D.; Kieling, A.G.; Brehm, F.A.; Rigon, M.R.; Berwanger Filho, J.A.; Schneider, I.A.H.; Osorio, E. Review of the rice production cycle: By-products and the main applications focusing on rice husk combustion and ash recycling. *Waste Manag. Res.* **2014**, *32*, 1034–1048. [CrossRef] [PubMed]
5. Satbaev, B.; Yefremova, S.; Zharmenov, A.; Kablanbekov, A.; Yermishin, S.; Shalabaev, N.; Satbaev, A.; Khen, V. Rice husk research: From environmental pollutant to a promising source of organo-mineral raw materials. *Materials* **2021**, *14*, 4119. [CrossRef] [PubMed]

6. Wang, C.-F. Study of the earth composition of adobe walls and bamboo-daub walls—A case study of traditional buildings, Yunlin County and Chiayi County. *J. Cult. Herit. Conserv.* **2020**, *52*, 7–26.
7. Rodríguez de Sensale, G. Strength development of concrete with rice-husk ash. *Cem. Concr. Compos.* **2006**, *28*, 158–160. [CrossRef]
8. Ramasamy, V. Compressive strength and durability properties of Rice Husk Ash concrete. *KSCE J. Civ. Eng.* **2012**, *16*, 93–102. [CrossRef]
9. Sandhu, R.K.; Siddique, R. Influence of rice husk ash (RHA) on the properties of self-compacting concrete: A review. *Constr. Build. Mater.* **2017**, *153*, 751–764. [CrossRef]
10. Madandoust, R.; Ranjbar, M.M.; Moghadam, H.A.; Mousavi, S.Y. Mechanical properties and durability assessment of rice husk ash concrete. *Biosyst. Eng.* **2011**, *110*, 144–152. [CrossRef]
11. Chao-Lung, H.; Anh-Tuan, B.L.; Chun-Tsun, C. Effect of rice husk ash on the strength and durability characteristics of concrete. *Constr. Build. Mater.* **2011**, *25*, 3768–3772. [CrossRef]
12. Chandrasekhar, S.; Satyanarayana, K.G.; Pramada, P.N.; Raghavan, P.; Gupta, T.N. Review processing, properties and applications of reactive silica from rice husk—An overview. *J. Mater. Sci.* **2003**, *38*, 3159–3168. [CrossRef]
13. Abah, E.O.; Ahamed, T.; Noguchi, R. Catalytic temperature effects on conversion efficiency of $PM_{2.5}$ and gaseous emissions from rice husk combustion. *Energies* **2021**, *14*, 6131. [CrossRef]
14. Duan, F.; Chyang, C.; Chin, Y.; Tso, J. Pollutant emission characteristics of rice husk combustion in a vortexing fluidized bed incinerator. *J. Environ. Sci.* **2013**, *25*, 335–339. [CrossRef] [PubMed]
15. Ataie, F. Influence of rice straw fibers on concrete strength and drying shrinkage. *Sustainability* **2018**, *10*, 2445. [CrossRef]
16. Pachla, E.C.; Silva, D.B.; Stein, K.J.; Marangon, E.; Chong, W. Sustainable application of rice husk and rice straw in cellular concrete composites. *Constr. Build. Mater.* **2021**, *283*, 122770. [CrossRef]
17. Muthukrishnan, S.; Gupta, S.; Kua, H.W. Application of rice husk biochar and thermally treated low silica rice husk ash to improve physical properties of cement mortar. *Theor. Appl. Fract. Mech.* **2019**, *104*, 102376. [CrossRef]
18. Ministry of Agriculture. *Taiwan's Pathway to Net-Zero Emissions in 2050-Carbon Sink*; Ministry of Agriculture: Taipei, Taiwan, 2023.
19. Chinnu, S.N.; Minnu, S.N.; Bahurudeen, A.; Senthilkumar, R. Reuse of industrial and agricultural by-products as pozzolan and aggregates in lightweight concrete. *Constr. Build. Mater.* **2021**, *302*, 124172. [CrossRef]
20. Narayanan, N.; Ramamurthy, K. Structure and properties of aerated concrete: A review. *Cem. Concr. Compos.* **2000**, *22*, 321–329.
21. Thienel, K.-C.; Haller, T.; Beuntner, N. Lightweight concrete—From basics to innovations. *Materials* **2020**, *13*, 1120. [CrossRef]
22. Hamad, A.J. Materials, production, properties and application of aerated lightweight concrete: Review. *Int. J. Mater. Sci. Eng.* **2014**, *2*, 152–157. [CrossRef]
23. Kalpana, M.; Mohith, S. Study on autoclaved aerated concrete: Review. *Mater. Today Proc.* **2020**, *22*, 894–896.
24. Rahman, R.A.; Fazlizan, A.; Asim, N.; Thongtha, A. Utilization of waste material for aerated autoclaved concrete production: A preliminary review. *IOP Conf. Ser. Earth Environ. Sci.* **2020**, *463*, 012035. [CrossRef]
25. Jauberthie, R.; Rendell, F.; Tamba, S.; Cisse, I. Origin of the pozzolanic effect of rice husks. *Constr. Build. Mater.* **2000**, *14*, 419–423. [CrossRef]
26. Kunchariyakun, K.; Asavapisit, S.; Sombatsompop, K. Properties of autoclaved aerated concrete incorporating rice husk ash as partial replacement for fine aggregate. *Cem. Concr. Compos.* **2015**, *55*, 11–16. [CrossRef]
27. Kunchariyakun, K.; Asawapisit, S.; Sombatsompop, K. The effect of rice husk ash on properties of aerated concrete. *Adv. Mater. Res.* **2013**, *747*, 420–423. [CrossRef]
28. Qin, L.; Gao, X.; Chen, T. Recycling of raw rice husk to manufacture magnesium oxysulfate cement based lightweight building materials. *J. Clean. Prod.* **2018**, *191*, 220–232. [CrossRef]
29. Winarno, S. Comparative Strength and cost of rice husk concrete block. *MATEC Web Conf.* **2019**, *280*, 04002. [CrossRef]
30. Akinyemi, B.; Omoniyi, T.E.; Elemile, O.; Arowofila, O. Innovative husk-crete building materials from rice chaff and modified cement mortars. *Acta Technol. Agric.* **2020**, *23*, 67–72. [CrossRef]
31. Akinwumi, I.I.; Awoyera, P.O.; Olofinnade, O.M.; Busari, A.A.; Okotie, M. Rice husk as a concrete constituent: Workability, water absorption and strength of the concrete. *Asian J. Civil Eng.* **2016**, *17*, 887–898.
32. Doumongue, B.; Limam, K.; Dany, A.Y.M.X.; Mastouri, H.; Bahi, H.; El bouazouli, A. Analysis of rice husk concrete samples observed by scanning electron microscopy. *Mater. Today Proc.* **2023**, *72*, 3850–3856. [CrossRef]
33. Chabannes, M.; Bénézet, J.-C.; Clerc, L.; Garcia-Diaz, E. Use of raw rice husk as natural aggregate in a lightweight insulating concrete: An innovative application. *Constr. Build. Mater.* **2014**, *70*, 428–438. [CrossRef]
34. Saeed, A.A.H.; Yub Harun, N.; Bilad, M.R.; Afzal, M.T.; Parvez, A.M.; Roslan, F.A.S.; Abdul Rahim, S.; Vinayagam, V.D.; Afolabi, H.K. Moisture content impact on properties of briquette produced from rice husk waste. *Sustainability* **2021**, *13*, 3069. [CrossRef]
35. Jamil, M.; Khan, M.N.N.; Karim, M.R.; Kaish, A.B.M.A.; Zain, M.F.M. Physical and chemical contributions of Rice Husk Ash on the properties of mortar. *Constr. Build. Mater.* **2016**, *128*, 185–198. [CrossRef]
36. Hossain, S.S.; Mathur, L.; Roy, P.K. Rice husk/rice husk ash as an alternative source of silica in ceramics: A review. *J. Asian Ceram. Soc.* **2018**, *6*, 299–313. [CrossRef]
37. Jittin, V.; Bahurudeen, A.; Ajinkya, S.D. Utilisation of rice husk ash for cleaner production of different construction products. *J. Clean. Prod.* **2020**, *263*, 121578. [CrossRef]

38. Liu, K.; Shen, C.; Wang, Y.; Rong, N.; Ma, J.; Wang, A.; Sun, D. The performance of autoclaved aerated concrete prepared by arenaceous rock coal gangue powder instead of fly ash: The effect of Ca/Si ratio. *Constr. Build. Mater.* **2024**, *441*, 137495. [CrossRef]
39. Peng, Y.; Liu, Y.; Zhan, B.; Xu, G. Preparation of autoclaved aerated concrete by using graphite tailings as an alternative silica source. *Constr. Build. Mater.* **2021**, *267*, 121792. [CrossRef]
40. Kumar, R. Effects of high volume dolomite sludge on the properties of eco-efficient lightweight concrete: Microstructure, statistical modeling, multi-attribute optimization through Derringer's desirability function, and life cycle assessment. *J. Clean Prod.* **2021**, *307*, 127107. [CrossRef]
41. Kurama, H.; Topçu, İ.B.; Karakurt, C. Properties of the autoclaved aerated concrete produced from coal bottom ash. *J. Mater. Process. Technol.* **2009**, *209*, 767–773. [CrossRef]
42. Lim, S.K.; Tan, C.S.; Lim, O.Y.; Lee, Y.L. Fresh and hardened properties of lightweight foamed concrete with palm oil fuel ash as filler. *Constr. Build. Mater.* **2013**, *46*, 39–47. [CrossRef]
43. Rahman, R.A.; Fazlizan, A.; Asim, N.; Thongtha, A. A review on the utilization of waste material for autoclaved aerated concrete production. *J. Renew. Mater.* **2021**, *9*, 61–72. [CrossRef]
44. Chen, Y.-L.; Chang, J.-E.; Lai, Y.-C.; Chou, M.-I.M. A comprehensive study on the production of autoclaved aerated concrete: Effects of silica-lime-cement composition and autoclaving conditions. *Constr. Build. Mater.* **2017**, *153*, 622–629. [CrossRef]
45. Qu, X.; Zhao, X. Previous and present investigations on the components, microstructure and main properties of autoclaved aerated concrete—A review. *Constr. Build. Mater.* **2017**, *135*, 505–516. [CrossRef]
46. Dong, M.; Ma, R.; Sun, G.; Pan, C.; Zhan, S.; Qian, X.; Chen, R.; Ruan, S. Size distribution of pores and their geometric analysis in red mud-based autoclaved aerated concrete (AAC) using regression neural network and elastic mechanics. *Constr. Build. Mater.* **2022**, *359*, 129420. [CrossRef]
47. *CNS 13480*; Autoclaved Lightweight Aerated Concrete Blocks. Bureau of Standards Metrology and Inspection: Taipei, Taiwan, 1995.